Particle-hole excitations within a self-consistent random-phase approximation

D. Gambacurta[1,2,*] and F. Catara[2,3,†]
[1]*Consortium COMETA, Via S. Sofia 64, I-95123 Catania, Italy*
[2]*Dipartimento di Fisica ed Astronomia dell'Università di Catania, Via S. Sofia 64, I-95123 Catania, Italy*
[3]*Istituto Nazionale di Fisica Nucleare, Sezione di Catania, Via S. Sofia 64, I-95123 Catania, Italy*
(Received 14 January 2008; revised manuscript received 2 April 2008; published 23 May 2008)

We present a method for the treatment of correlations in finite Fermi systems in a more consistent way than the random phase approximation (RPA). The main differences with respect to previous approaches are underlined and discussed. In particular, no use of renormalized operators is made. By means of the method of linearization of equations of motion, we derive a set of RPA-like equations depending only on the one-body density matrix. The latter is no more assumed to be diagonal and it is expressed in terms of the X and Y amplitudes of the particle-hole phonon operators. This set of nonlinear equations is solved via an iterative procedure, which allows us to calculate the energies and the wave functions of the excited states. After presenting our approach in its general formulation, we test its quality by using metal clusters as a good test laboratory for a generic many-body system. Comparison to RPA shows significant improvements. We discuss also how the present approach can be further extended beyond the particle-hole configuration space, getting an approximation scheme in which energy weighted sum rules are exactly preserved, thus solving a problem common to all extension of RPA proposed until now. The implementation of such approach will be afforded in a future work.

DOI: 10.1103/PhysRevB.77.205434 PACS number(s): 21.60.Jz, 21.10.Pc, 21.10.Re

I. INTRODUCTION

The advent of modern computers and the continuous improvement of their performances, together with the increasing ability to exploit them by using more and more refined algorithms, has made possible to calculate quite accurately the properties of ground state and low energy excited states of many-body systems starting from the basic interaction[1] within several methods: no-core shell model,[2–4] coupled cluster,[5–8] and the Green's function Monte Carlo[9–12] calculations. However, it is not clear whether in the near future an accurate description of higher lying states can be achieved along such paths. Another microscopic approach, particularly well suited for the study of collective vibrational states, is based on the Hartree–Fock (HF) plus random phase approximation (RPA) with an effective interaction derived from the density-energy functional.[13–15] As it is well known, in the HF approximation, one imposes that the ground state of the system is the Slater determinant minimizing the expectation value of the Hamiltonian. By solving the corresponding variational equations, one gets the "best" single particle wave functions by which that Slater determinant is built. A complete single particle basis is then determined by solving the one-body Schrödinger equation with the self-consistent HF potential, both for the states occupied in the ground state (holes) and the unoccupied ones (particles). The excited states are then studied within the RPA, describing them as superpositions of particle-hole (p-h) configurations, built on top of the unknown exact ground state including correlations. However, RPA, while having several very nice properties[14,15] and being completely microscopic, contains some approximations. In fact, since the explicit structure of the correlated ground state is not known, the standard RPA is obtained by replacing, in the evaluation of the matrix elements of the RPA equations, this state by the uncorrelated HF one. The replacement, also called quasiboson approximation, produces a missing of some terms in the evaluation of the commutators in the equations of motion and thus a violation of Pauli principle. Various attempts have been done to improve over them or by using boson expansion methods,[16–24] or remaining entirely in the fermionic space.[25–37] In Ref. 32, an extension of RPA, named improved RPA (IRPA), was presented. The starting point was the introduction of renormalized p-h operators and, by using the method of linearization of the equations of motion, a set of nonlinear RPA-like equations was obtained. The main drawback of IRPA is the fact that one assumes the one-body density matrix (OBDM) to be diagonal in the HF basis. Such limit was eliminated in Ref. 33, where a more refined procedure was used. In the present paper, we move along the line of Refs. 32 and 33 and introduce a more general approach, which we will call extended RPA (ERPA) for brevity, not based on the renormalized RPA (RRPA). We will also show some results obtained by applying this method to the study of the excitation spectrum and other properties of metallic clusters within the uniform jellium model[38,39] with bare Coulomb interaction both for the electrons with the jellium and for the electrons among themselves.[40] We are aware that the jellium approximation is too poor for a quantitative study; on the other hand, our purpose here is not to make a realistic study of metal clusters but rather to compare different levels of approximations. In fact, we believe that such a model is a very good test laboratory since it contains many characteristics of a generic realistic many-body system and, on the other hand, it allows a more clear comparison among different approaches because no adjustable parameter is present in it (as it is often the case with effective interactions). We stress that the present approach can be used to study any many-body system, the only differences being the interaction and the relevant quantum numbers. In particular, we plan to apply it to nuclei where, for example, RRPA has been shown to improve the descrip-

tion of double beta decay with respect to RPA.[41,42]

As discussed in Secs. II and III, the merits of the present approach with respect to previous ones[32,33] can be traced back to the fact that one does not move anymore in the RRPA scheme. On the other hand, the problem remains that, as in all the extensions of RPA proposed until now, violations of the energy weighted sum rules (EWSRs) are still present. In this respect, we recall that the fulfillment of EWSR guarantees that spurious excitations corresponding to broken symmetries as, for example, the translational invariance, separate out and are orthogonal to the physical states. We show that by enlarging the configuration space, along the lines of Ref. 37, within the present framework, it should be possible to implement a completely self-consistent RPA preserving the EWSR and to overcome the difficulties pointed out in Ref. 37 where the RRPA enlarged scheme was studied in a three-level Lipkin model. This possibility will be investigated in the near future.

In Sec. II, the basic equations of ERPA are shown and their derivation is outlined, while Sec. III is devoted to transition amplitudes and sum rules. In Sec. IV, we show the results and compare them with the RPA ones and with the available experimental data. An improved agreement with the latter is obtained. Finally, in Sec. V, we draw the main conclusions and outline the direction for future work.

II. BASIC EQUATIONS OF ERPA

In Ref. 32, an extension of RPA, named IRPA, was presented. The starting point was to introduce renormalized p-h creation and annihilation operators (for notation simplicity, we do not indicate coupling to total quantum numbers),

$$B_{ph}^{\dagger} = \sum_{p'h'} N_{ph,p'h'} a_{p'}^{\dagger} a_{h'} \tag{1}$$

by which one builds the operators

$$Q_{\nu}^{\dagger} = \sum_{ph} (X_{ph}^{\nu} B_{ph}^{\dagger} - Y_{ph}^{\nu} B_{ph}), \tag{2}$$

whose action on the ground state of the system $|0\rangle$ generates the collective states,

$$|\nu\rangle = Q_{\nu}^{\dagger}|0\rangle, \tag{3}$$

with $|0\rangle$ defined as the vacuum of the Q_{ν}'s,

$$Q_{\nu}|0\rangle = 0. \tag{4}$$

By assuming that the one-body density matrix is diagonal

$$\langle 0|a_{\alpha}^{\dagger} a_{\beta}|0\rangle = n_{\alpha}\delta_{\alpha\beta}, \tag{5}$$

choosing

$$N_{ph,p'h'} = \delta_{pp'}\delta_{hh'}(n_h - n_p)^{-1/2} \equiv \delta_{pp'}\delta_{hh'}D_{ph}^{-1/2}, \tag{6}$$

and following the equations of motion method,[14,15] one finds for the excitation energies ω_{ν} and the X and Y amplitudes,

$$\begin{pmatrix} A & B \\ -B^{*} & -A^{*} \end{pmatrix} \begin{pmatrix} X^{(\nu)} \\ Y^{(\nu)} \end{pmatrix} = \omega_{\nu} \begin{pmatrix} X^{(\nu)} \\ Y^{(\nu)} \end{pmatrix}, \tag{7}$$

with

$$A_{ph,p'hp} = \langle 0|[B_{ph}, H, B_{p'h'}^{\dagger}]|0\rangle, \tag{8}$$

and

$$B_{ph,p'hp} = -\langle 0|[B_{ph}, H, B_{p'h'}]|0\rangle, \tag{9}$$

where H is the Hamiltonian of the system and the symmetrized double commutators are defined as

$$[A,B,C] = \frac{1}{2}\{[A,[B,C]] + [[A,B],C]\}. \tag{10}$$

In IRPA, the X and Y amplitudes satisfy the same orthonormality conditions as in RPA,

$$\sum_{ph} (X_{ph}^{\nu} X_{ph}^{\nu'} - Y_{ph}^{\nu} Y_{ph}^{\nu'}) = \delta_{\nu\nu'}, \tag{11}$$

following from Eqs. (4)–(6). In order to make affordable the solution of Eqs. (7), one has to resort to some approximation. In IRPA, the linearization of the equations of motion was used: all the two-body terms appearing in the commutator of the Hamiltonian with a p-h operator are contracted with respect to the reference state $|0\rangle$. In this way, one obtains a quantity linear in the p-h operators. Substituting this in the double commutators of Eqs. (8) and (9), one gets an expression for the matrices $A_{ph,p'h'} = \langle 0|[a_h^{\dagger}a_p, H, a_{p'}^{\dagger}a_{h'}]|0\rangle$ and B containing only the OBDM. The standard RPA equations can be derived by the same procedure but using the uncorrelated HF ground state instead of the correlated one $|0\rangle$. In the IRPA case, this method leads to a set of RPA-like equations, but with the A and B matrices depending on the occupation numbers which, in turn, can be evaluated in terms of the X and Y amplitudes by using the number operator method.[43] The equations of motion are thus nonlinear and have been solved iteratively. One limitation of IRPA is the fact that one assumes the OBDM to be diagonal in the HF basis. Such inconsistency was eliminated in Ref. 33, where a double iterative procedure was used: starting from a zero order approximation and assuming the OBDM to be diagonal, one solves the IRPA equations, next the number operator method is used to calculate the OBDM with the so determined X and Y, then the OBDM is diagonalized and the IRPA calculation is repeated in the new basis, and so on until convergence is reached. Of course, this double iterative procedure is quite demanding from the computational point of view. On the other hand, use is still made of ansatz (1) and choice (6). This is certainly a limitation. In the following, we will present an improved approach (ERPA), in which such a limitation is overcome. Thus, ERPA is completely self-consistent within the linearization of the equations of motion method.

In the present approach, after the single particle basis is fixed by solving the HF equations, we introduce phonon operators Q_{ν} having the same form as the RPA ones,

$$Q_{\nu}^{\dagger} = \sum_{ph} (X_{ph}^{\nu} a_p^{\dagger} a_h - Y_{ph}^{\nu} a_h^{\dagger} a_p), \tag{12}$$

avoiding thus the use of "renormalized" operators and choice (6).

The X and Y amplitudes are solutions of the system of equations

$$\begin{pmatrix} A & B \\ B^* & A^* \end{pmatrix}\begin{pmatrix} X^{(\nu)} \\ Y^{(\nu)} \end{pmatrix} = \omega_\nu \begin{pmatrix} G & 0 \\ 0 & -G^* \end{pmatrix}\begin{pmatrix} X^{(\nu)} \\ Y^{(\nu)} \end{pmatrix}, \tag{13}$$

where

$$A_{ph,p'h'} = \langle 0|[a_h^\dagger a_p, H, a_{p'}^\dagger, a_{h'}]|0\rangle, \tag{14}$$

$$B_{ph,p',h'} = -\langle 0|[a_h^\dagger a_p, H, a_{h'}^\dagger, a_{p'}]|0\rangle, \tag{15}$$

$$G_{ph,p',h'} = \langle 0|[a_h^\dagger a_p, a_{p'}^\dagger, a_{h'}]|0\rangle, \tag{16}$$

and satisfy the orthonormality conditions

$$\sum_{ph,p'h'} (X_{ph}^{v} X_{p'h'}^{v'} - Y_{ph}^{v} Y_{p'h'}^{v'}) G_{ph,p'h'} = \delta_{vv'}. \tag{17}$$

The standard RPA equations can be obtained by replacing, in the evaluation of matrices (14)–(16), the state $|0\rangle$ with the (uncorrelated) HF one. In particular, the norm matrix G acquires the simpler form

$$G_{ph,p',h'}^{(\mathrm{HF})} = \langle \mathrm{HF}|[a_h^\dagger a_p, a_{p'}^\dagger, a_{h'}]|\mathrm{HF}\rangle = \delta_{hh'}\delta_{pp'}, \tag{18}$$

and thus for the RPA X and Y amplitudes, we find again the orthonormality conditions (11). This substitution introduces a visible inconsistency since, on one hand, the definition of ground state (4) as the vacuum of the Q operators is used to derive the Eqs. (13), while, on the other hand, the HF state is used in calculating the expectation values appearing in those equations. Furthermore, it introduces some violations of the Pauli principle.[15]

The explicit form of the ERPA matrices A, B, and G in terms of the OBDM ρ, obtained by using the linearization of the equations of motion, is

$$\begin{aligned} A_{ph,p'h'} = \frac{1}{2}\{&\rho(h,h')\epsilon(p,p') + \rho(p,p')\epsilon(h,h') \\ &- \delta_{hh'}\sum_{p_1}\rho(p,p_1)\epsilon(p_1,p') - \delta_{pp'}\sum_{h_1}\rho(h,h_1)\epsilon(h_1,h') \\ &+ \sum_{h_1h_2}\langle ph_1|v|h_2p'\rangle\rho(h_1,h')\rho(h_2,h) \\ &+ \sum_{p_1p_2}\langle hp_1|v|p_2h'\rangle\rho(p_1,p')\rho(p_2,p) \\ &+ 2\sum_{h_1p_1}\langle h_1p_1|v|p'h\rangle\rho(h_1,h')\rho(p_1,p) \\ &+ (ph \leftrightarrow p'h')\}, \end{aligned} \tag{19}$$

$$\begin{aligned} B_{ph,p'h'} = -\{&\sum_{h_1h_2}\langle h_1h_2|v|p'p\rangle\rho(h_1,h')\rho(h_2,h) \\ &+ \sum_{p_1p_2}\langle h'h|v|p_1p_2\rangle\rho(p_1,p')\rho(p_2,p) \\ &+ \sum_{h_1p_1}\langle h_1h|v|p_1p'\rangle\rho(h_1,h')\rho(p_1,p) \\ &+ \sum_{h_1p_1}\langle h_1h'|v|p_1p\rangle\rho(h_1,h)\rho(p_1,p')\}, \end{aligned} \tag{20}$$

$$G_{ph,p'h'} = \delta_{pp'}\rho(h,h') - \delta_{hh'}\rho(p,p'), \tag{21}$$

where t and v are the one-body and the two-body parts of the Hamiltonian, respectively.

In Eq. (19), the ϵ quantities are defined as

$$\epsilon(\alpha,\beta) = t_{\alpha,\beta} + \sum_{\gamma\delta}\langle\alpha\gamma|v|\beta\delta\rangle\rho(\gamma,\delta), \tag{22}$$

in which α, β, γ, and δ run over all single particle states. Note that when $\rho(\alpha,\beta)$ is assumed to be diagonal and its eigenvalues equals to 0 or 1, i.e., in the HF limit, the above quantities become

$$\epsilon(\alpha,\beta) = t_{\alpha,\beta} + \sum_h \langle\alpha h|v|\beta h\rangle \equiv \langle\alpha|H_{HF}|\beta\rangle, \tag{23}$$

where H_{HF} is the HF one-body Hamiltonian. Since the latter commutes with the HF one-body density, $\epsilon(\alpha,\beta) = \epsilon_\alpha\delta(\alpha,\beta)$, where ϵ_α are the HF single particle energies. The matrix $\epsilon(\alpha,\beta)$ of Eq. (22) can be diagonalized without going to the HF limit using instead the OBDM obtained self-consistently within ERPA. In this way, one gets a kind of "generalized single particle energies." We will discuss that in Sec. IV.

In the expressions for the A, B, and G matrices, the OBDM appears. By using the number operator method,[43] its matrix elements are expressed in terms of the X and Y amplitudes. Therefore, Eqs. (13) are nonlinear. In the present approach, we have

$$\rho(p,h) \equiv \langle 0|a_p^\dagger a_h|0\rangle = 0, \tag{24}$$

$$\begin{aligned} \rho(p,p') \equiv \langle 0|a_p^\dagger a_{p'}|0\rangle = \sum_{\nu\nu'} S(\nu,\nu')\sum_{p_1h_1}\sum_{p_2h_2} Y_{p_1h_1}^{\nu} Y_{p_2h_2}^{\nu'*} \\ \times \sum_h G(ph,p_1h_1)G^*(p'h,p_2h_2), \end{aligned} \tag{25}$$

$$\begin{aligned} \rho(h,h') \equiv \langle 0|a_h^\dagger a_{h'}|0\rangle = \delta_{hh'} - \sum_{\nu\nu'} S(\nu,\nu')\sum_{p_1h_1}\sum_{p_2h_2} Y_{p_1h_1}^{\nu} Y_{p_2h_2}^{\nu'*} \\ \times \sum_p G(ph,p_1h_1)G^*(ph',p_2h_2), \end{aligned} \tag{26}$$

where

$$\begin{aligned} S(\nu,\nu') = \delta_{\nu\nu'} - \frac{1}{2}\sum_{p_1h_1,p_2h_2} X_{p_1h_1}^{\nu} X_{p_2h_2}^{\nu'*} \\ \times \sum_{p_3h_3} G(p_3h_3,p_1h_1)G^*(p_3h_3,p_2h_2). \end{aligned} \tag{27}$$

The above equations are exact up to order $O(|Y|^4)$. We remark that in Eqs. (25) and (26), the X and Y amplitudes as well as the norm matrix G appear. In order to solve the equations of motions (13), we use an iterative procedure. At the nth iterative step, we compute the ρ matrix, and thus, the A, B, and G matrices by using the X and Y amplitudes and the ρ matrix of the $(n-1)$th step. As starting point, we take the solutions of the standard RPA equations and the HF ρ matrix. This procedure is carried out until convergence is reached.

In the present approach, all calculations are carried out in the HF single particle basis. The OBDM is calculated in the correlated ground state $|0\rangle$ state defined as the vacuum of the Q operators. Another possible choice could be to work in the basis which diagonalizes OBDM (as it was made in Ref. 33 in the RRPA approach) or the "generalized single particle energies" [Eq. (22)]. In both cases, at each step of the iterative procedure, one has to diagonalize ρ or ϵ matrix and, after that, calculate the G, A, and B matrices in the new basis. These operations make the procedure more cumbersome from a numerical point of view.

III. TRANSITION AMPLITUDES AND SUM RULES

As it is well known, if $|0\rangle$ and $|\nu\rangle$ are a complete set of exact eigenstates of the Hamiltonian, with eigenvalues E_0 and E_ν, the following identity holds:

$$\sum_\nu \omega_\nu |\langle \nu|F|0\rangle|^2 = \frac{1}{2}\langle 0|[F,[H,F]]|0\rangle, \tag{28}$$

where $\omega_\nu = E_\nu - E_0$. The above equality is in general violated to some extent when $|0\rangle$, $|\nu\rangle$, and ω_ν are calculated with some approximation. To which extent it is satisfied is a measure of the adequacy of the approximation. We note that the right-hand side is a quantity which depends only on the ground state properties.

Let us examine the transition amplitudes $\langle \nu|F|0\rangle$ induced by a one-body operator,

$$F = \sum_{\alpha,\beta} \langle \alpha|F|\beta\rangle a_\alpha^\dagger a_\beta, \tag{29}$$

between the ground state $|0\rangle$ and excited states $|\nu\rangle$. By using definition (3) and the vacuum property (4), one gets

$$\langle \nu|F|0\rangle = \langle 0|[Q_\nu, F]|0\rangle. \tag{30}$$

The above expression is general and it is valid independently of the explicit form of the Q operators. When the latter has form (12), only the p-h components of the transition operator F are selected. A very important feature of RPA, known as Thouless theorem,[44] can be described as follows. In both sides of Eq. (28), the HF state is used, instead of the correlated $|0\rangle$ one. Then, from Eq. (30), one gets

$$\langle \nu|F|0\rangle = \sum_{ph} \{X_{ph}^{\nu *}\langle p|F|h\rangle + Y_{ph}^{\nu *}\langle h|F|p\rangle\}. \tag{31}$$

i.e., the standard RPA expression. On the other hand, the right-hand side evaluated in the HF state can be completely expressed in terms of the A and B matrices of RPA. It is then easy to show[15,44] that, if the left-hand side is calculated by using Eq. (31) and the RPA values for the energies ω_ν and the X^ν and Y^ν amplitudes, equality (28) is exactly satisfied. This result is very important also because it guarantees that spurious excitations corresponding to broken symmetries (as, for example, the translational invariance) separate out and are orthogonal to the physical states. We remark that, when the right-hand side is evaluated in the HF state, only the p-h components of the transition operator F appear in it.

When the correlated $|0\rangle$ is maintained, it is still true that only the p-h components of the transition operator F appear on the left-hand side and one has

$$\langle \nu|F|0\rangle = \sum_{php'h'} \{X_{ph}^{\nu *}\langle p'|F|h'\rangle + Y_{ph}^{\nu *}\langle h'|F|p'\rangle\} G_{ph,p'h'}, \tag{32}$$

while this is no more the case on the right-hand side, where the whole structure of F appears. This is the reason why all extensions of RPA, with only p-h excitations, violate Eq. (28). We stress that if only the p-h part of the F operator is taken in the double commutator and the latter is calculated by the linearization procedure, just the ERPA matrices A, B, and G appear on the right-hand side. Therefore, if ERPA quantities are used also on the left-hand side, the EWSR is preserved.

Since the deviations present in ERPA can be ascribed to the fact that the $Q_\nu^\dagger$ operators have the structure of Eq. (12), a possible generalization would be to assume

$$Q_\nu^\dagger = \sum_{\alpha>\beta} (X_{\alpha\beta}^\nu a_\alpha^\dagger a_\beta - Y_{\alpha\beta}^\nu a_\beta^\dagger a_\alpha) \tag{33}$$

where α and β denote generic single particle states (occupied and not). As shown in Ref. 37 within such "enlarged" RPA approach, equality (28) holds exactly. This has been also tested numerically in Ref. 37 where an enlarged RRPA approach has been applied to a three-level Lipkin model. However, a difficulty was pointed out, namely, the appearance of a nonphysical state, which could not be eliminated within that approach. Within the RRPA, such state could not be identified *a priori* but, by comparison, it was found that it did not correspond to any exact eigenstate. In a realistic calculation, of course, this is not possible. In the scheme we are presenting in this paper, this difficulty may be overcome since nonphysical states, if any, can be singled out by looking for zero eigenvalues of the norm matrix G, thus getting, within the method of linearization of the equations of motion, a self-consistent approach. This will be the subject of future investigations.

IV. RESULTS AND DISCUSSION

As mentioned above, the described method can be used to study any many-body system. In this section, we apply it to study the electronic properties of metal clusters. In fact, such systems show many characteristics of a generic realistic many-body system and, on the other hand, a more clear comparison among different approaches can be done since no resort to effective interactions, depending on adjustable parameters, is necessary.

The ERPA results will be compared with those obtained in the standard RPA approach. The calculations are done in the jellium approximation. In this model, the ionic background is described as a uniform positive charge distribution, which interacts with the delocalized valence electrons, also interacting among themselves, via the bare Coulomb interaction. The jellium properties are completely determined by one parameter, the Wigner–Seitz radius r_s. Within this model, the

motion of the valence electrons is determined by the Hamiltonian

$$H = \sum_i h_i + \sum_{i<j} v_{ij}, \tag{34}$$

with

$$h_i = -\frac{\hbar^2}{2m}\nabla_i^2 + V(r_i); \quad v_{ij} = \frac{e^2}{4\pi}\frac{1}{|\vec{r}_i - \vec{r}_j|}, \tag{35}$$

and

$$V(r) = \frac{Ze^2}{4\pi}\begin{cases} (1/2r_c)(r^2/r_c^2 - 3) & \text{for } r \le r_c \\ -1/r & \text{for } r \ge r_c, \end{cases} \tag{36}$$

where N_e is the number of electrons and r_c is the radius of the jellium sphere, i.e., $r_c = r_s N_e^{1/3}$.

The procedure that we have followed consists of the following steps. First of all, we have obtained, by solving HF equations, the single particle basis, in which all the subsequent calculations are carried out. The single particle wave functions have been represented as linear superposition of harmonic oscillator ones. After that, we have solved the standard RPA equations. The so obtained X and Y amplitudes are used as input quantities in the ERPA iterative procedure. In the first step, we thus use them and the HF norm matrix (18) to calculate the OBDM. With the new A, B, and G matrices, we solve the ERPA [Eq. (13)]. The new X's and Y's and the G matrix of the previous iterative step are used to recalculate the OBDM and so on until convergence is reached, namely, until the maximum relative difference in the excitations energies between two successive iterations is less than a chosen limit. In the calculations, we are going to present that this limit has been put equal to 10^{-5}.

We remark that, at each step of the iterative procedure, we solve the ERPA equations for multipolarities ranging from $L=0$ to $L=6$ for both the spin $S=0$ and $S=1$ channels, and the so obtained X and Y amplitudes, for all L and S, are used in building the new OBDM. At RPA level, in some cases, these equations are found to have imaginary solutions. This happens, for example, for some states with spin $S=1$ and it is due to the too much attractive behavior of the bare Coulomb interaction in the $S=1$ channel. The states having imaginary energies are thus not included in the initial steps. However, with the use of the new OBDM, we find that the final solutions are real for all L and S states.

The present approach has been applied to the study of neutral and ionized closed shell Na clusters, with a number of valence electrons ranging from 8 to 92. However, in the following, we will focus our analysis on the medium-size Na_{40} and Na_{41}^+ clusters since the qualitative behavior is the same for the other closed shell clusters.

In Fig. 1, we show the centroid energies of the strength distributions for multipolarities from $L=0$ to $L=4$ and spin $S=0$ and $S=1$ in Na_{40}. In each panel, the values on the left and on the right-hand sides are those obtained in RPA and ERPA, respectively. Note that for $S=1$ and $L=3$, RPA collapses. The differences among the two approaches are quite pronounced in both the $S=0$ and the $S=1$ spin channels. In the latter case, we see that all the centroids are pushed up as

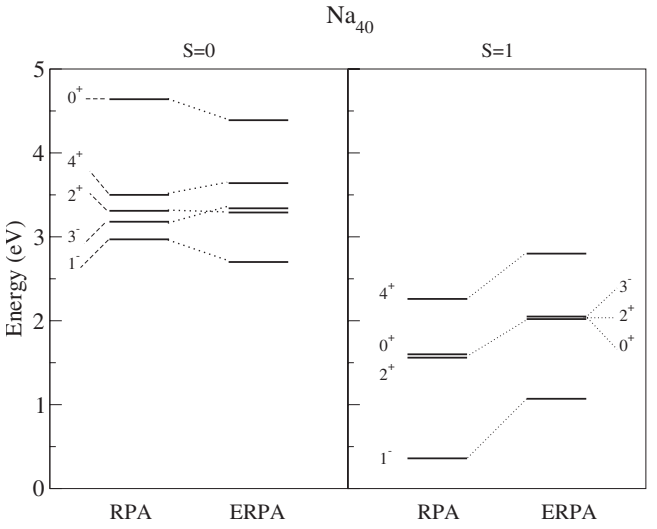

FIG. 1. RPA and ERPA centroid energies (eV) of Na_{40} cluster for multipolarities from $L=0$ to $L=4$ and spin $S=0$ (left panel) and $S=1$ (right panel).

a consequence of the better treatment of ground state correlations in ERPA with respect to RPA. In particular, the collapse of RPA for $L=3$ is not present in ERPA.

In Figs. 2 and 3, we plot the dipole strength distributions obtained by folding the discrete lines of RPA and ERPA spectra with a Lorentzian function. In both cases, an artificial width $\Gamma=0.1$ eV has been used. In Fig. 2, we show the $S=0$ dipole strength distribution for the neutral case. The solid line refers to the calculations performed within the present approach, whereas the dashed line to those of standard RPA. The experimental distribution[45] exhibits two broad peaks at about 2.4 and 2.65 eV and the first one is higher than the second one. As we can observe in Fig. 2, RPA predicts the first peak at an energy of about 2.45 eV, very close to the experimental value, and the second one much higher, at about 2.97 eV. Furthermore, the height of the second peak is about twice that of the first one. In ERPA, both peaks are

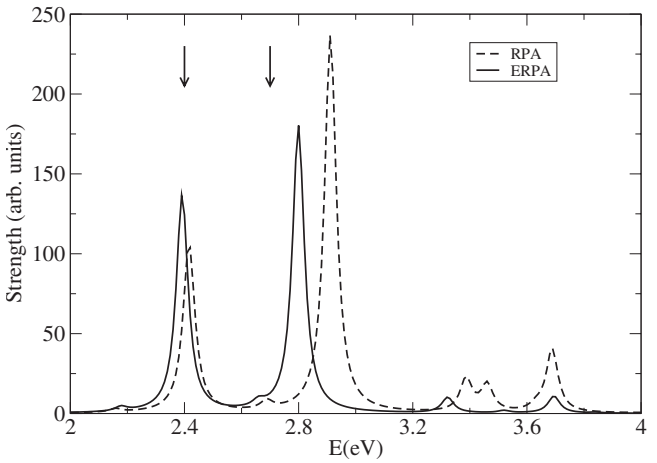

FIG. 2. Spin=0 dipole strength for Na_{40} metal cluster. The solid line refers to calculations performed within the present approach, while the dashed line refers to standard RPA calculations. The arrows roughly indicate the positions of the experimental peaks.

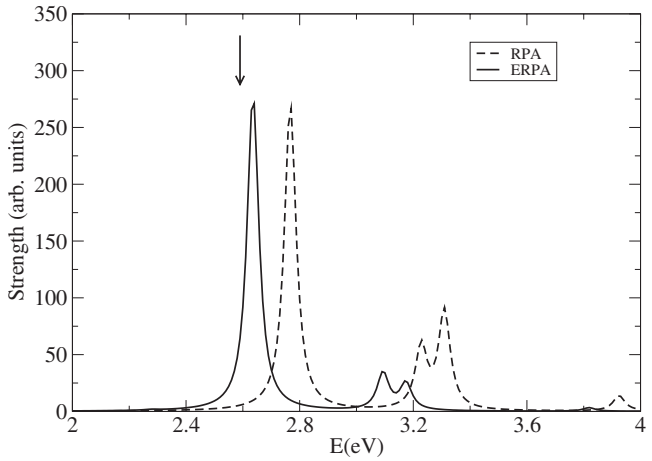

FIG. 3. As in Fig. 2 but for Na_{41}^{+} metal cluster.

shifted to lower energies, at about 2.39 and 2.79 eV, in agreement with the experimental values (indicated by arrows in the figure). Also, the structure of the distribution changes and a reshuffling of the strength, qualitatively in better agreement with the experimental results, are observed. In particular, we have an increasing of the height of the first peak and a lowering of the second one. However, the strength distribution remains quite different from the experimental one. In Fig. 3, we show the $S=0$ dipole strength distribution for the ionized cluster Na_{41}^{+}. Also, in this case, the calculated distribution is shifted with respect to the RPA results and it fits well with the experimental results,[46] in which a single peak at about 2.6 eV is found. The ERPA energy of this peak is about 2.64 eV, rather better than the RPA one which lies at about 2.77 eV. The improvement obtained in ERPA can be seen by analyzing also the centroid energy associated with the strength distribution. The ERPA result (2.70 eV) is lower by ~10% with respect to the RPA one (2.97 eV), quite close to the experimental value (2.62 eV).[46]

If F is a multipole operator $r^{\lambda}Y_{\lambda 0}$ and the Hamiltonian contains a kinetic energy term plus a local two-body interaction, one gets[15]

$$\frac{1}{2}\langle 0|[F,[H,F]]|0\rangle = \frac{\hbar^2}{2m}\frac{\lambda(2\lambda+1)}{4\pi}N\langle 0|r^{2\lambda-2}|0\rangle, \quad (37)$$

with N as the number of particles and

$$\langle 0|r^{2\lambda-2}|0\rangle = \frac{1}{N}\sum_{\alpha,\beta}\rho(\alpha,\beta)\int r^{2\lambda-2}\varphi_{\alpha}(r)\varphi_{\beta}^{*}(r)d^3r, \quad (38)$$

where α and β stand for any single particle states with wave functions $\varphi_{\alpha}(r)$ and $\varphi_{\beta}(r)$.

Let us now consider some results on the sum rules. As we discussed in Sec. III, Eq. (28) is an identity when a complete set of exact eigenstates of the Hamiltonian is used. Therefore, analyzing the deviations from equality when different approximate schemes are used is a good test to verify and to compare their adequacy. We recall again that the Thouless theorem states that Eq. (28) is exactly satisfied if the mean values in the correlated ground state $|0\rangle$, appearing in both sides are approximated by those in the $|\mathrm{HF}\rangle$ one. When the mean values are calculated in the correlated ground state rather than in the HF one, some differences are expected. In Table I, we show, for Na_{40} and multipolarities ranging from 0 to 3, the values of the right-hand side of Eq. (28) calculated by using Eqs. (37) and (38) in the HF, RPA, and ERPA ground states and, correspondingly, the left-hand side calculated by using Eq. (32) with the HF, RPA, and ERPA one-body density. As above discussed, in standard RPA, the $|\mathrm{HF}\rangle$ state, and thus the HF one-body density, is used in evaluating the RPA matrices. On the other hand, the RPA ground state, defined as the vacuum of the Q operators, can be explicitly obtained[15] within the quasiboson approximation. It has the form

TABLE I. For each multipolarity λ, we report the values of the two sides of Eq. (28), in units of $\text{Å}^{2\lambda}\cdot\text{eV}$, calculated in the HF (first row), RPA (second row), and ERPA (third row) ground states (GS). The right-hand side is calculated by using Eqs. (37) and (38), while the left-hand side by means of Eq. (32). Equations (24)–(26) and (42)–(44) are used in the ERPA and RPA case, respectively. The results refer to Na_{40}.

Multipolarity	Left-hand side	Right-hand side
	$\lambda=0$	
(HF GS)	0.16253×10^{4}	0.16199×10^{4}
(RPA GS)	0.55083×10^{3}	0.23964×10^{4}
(ERPA GS)	0.12819×10^{4}	0.16551×10^{4}
	$\lambda=1$	
(HF GS)	0.10960×10^{3}	0.10951×10^{3}
(RPA GS)	0.14767×10^{2}	0.10951×10^{3}
(ERPA GS)	0.76098×10^{2}	0.10951×10^{3}
	$\lambda=2$	
(HF GS)	0.20282×10^{5}	0.20239×10^{5}
(RPA GS)	0.61385×10^{4}	0.29955×10^{5}
(ERPA GS)	0.15843×10^{5}	0.20703×10^{5}
	$\lambda=3$	
(HF GS)	0.25643×10^{7}	0.25517×10^{7}
(RPA GS)	0.96030×10^{6}	0.83273×10^{7}
(ERPA GS)	0.20333×10^{7}	0.26591×10^{7}

$$|\mathrm{RPA}\rangle \propto e^{\hat{Z}}|\mathrm{HF}\rangle, \quad (39)$$

with

$$\hat{Z} = \frac{1}{2}\sum_{p_1h_1p_2h_2} Z_{p_1h_1p_2h_2}a_{p_1}^{\dagger}a_{h_1}a_{p_2}^{\dagger}a_{h_2}. \quad (40)$$

where the Z matrix satisfies the following relation:

$$Z = Y^{*}X^{*^{-1}}. \quad (41)$$

By using the number operator method of Ref. 43, one gets

$$\rho^{RPA}(\alpha,\beta) = n_{\alpha}\delta_{\alpha\beta}, \quad (42)$$

with

$$n_h = 1 - \frac{1}{2}\sum_{p,\nu} |Y^{\nu}_{ph}|^2, \tag{43}$$

and

$$n_p = \frac{1}{2}\sum_{h,\nu} |Y^{\nu}_{ph}|^2. \tag{44}$$

We remark that the above expressions for the occupation numbers differ from those obtained by making use of the QBA by the factor of $\frac{1}{2}$. The same result was obtained in Ref. 47.

From the first rows of Table I, we see that the Thouless theorem [i.e., equality of the left-hand side and right-hand side of Eq. (28) when both are calculated in $|\mathrm{HF}\rangle$] is numerically well satisfied, better than 1%, for the shown multipolarities. From the second and third rows, respectively, we see that both in RPA and ERPA, equality (28) is not satisfied. However, in the latter approach, the deviations are much smaller than those found when the RPA correlated ground state, and the corresponding X and Y amplitudes are used.

Another important quantity is the static dipole polarizability α that is related to the inverse moment,

$$S_{-1} = \sum_{\nu} \omega_{\nu}^{-1} |\langle \nu | F | 0 \rangle|^2, \tag{45}$$

by

$$S_{-1} = \frac{1}{2}\alpha. \tag{46}$$

In the case of Na_{40}, our RPA value is 522.42 $Å^3$, in very good agreement with that found in Ref. 40. The ERPA value is somewhat smaller, namely, 434.34 $Å^3$, to be compared with the experimental value of 605.46 ± 11.40 $Å^3$.[48] In this respect, however, it has to be noted that, as stressed also in Ref. 49, the jellium approximation may be too poor. Indeed, in Ref. 50, it is shown that the inclusion of ionic structure effects by means of pseudopotentials leads to an increase of 30% in the polarizability.

A problem encountered when RPA is applied to the study of nuclear systems is that the energies of the low lying states are found quite higher than the experimental values. This is related to the fact that the equations of motion contain the single particle HF energies, whose spacing is too large, especially the gap between the last occupied and the first unoccupied levels. As said at the end of Sec. II, in the ERPA equations of motion the quantities $\epsilon(\alpha,\beta)$ defined in Eq. (22) appear instead of the HF energies. In order to disentangle how much the modifications of the energies of the collective states are related to this, we have diagonalized $\epsilon(\alpha,\beta)$. In Fig. 4, the so obtained generalized single particle energies are compared with the HF ones. The main difference is that the states above the Fermi level are lowered while those below are pushed up. This might be one of the reasons why the energies of the collective states in ERPA are lower than those in RPA. It would be interesting to see how much this reduced gap can improve the results in nuclei.

In Fig. 5, we show the occupation numbers n_p for particle states and the opposite of the depletion numbers $n_h - 1$ for

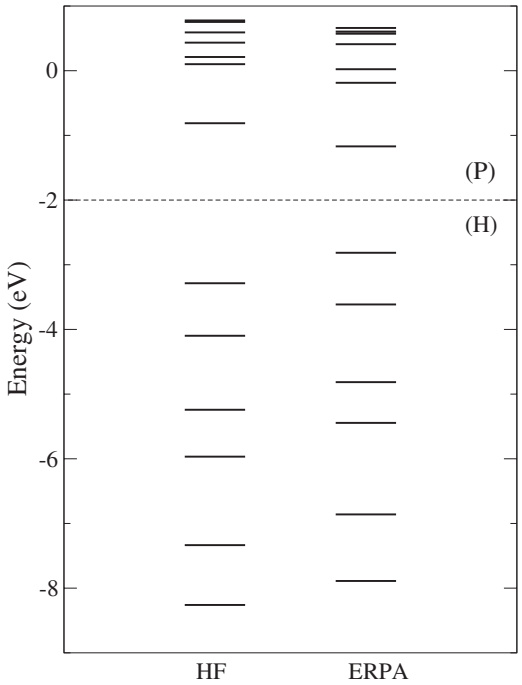

FIG. 4. HF single particle energies (left side) and generalized single particle ones (right side) (see the text for more details). A few lowest particle states (p) and the hole ones (h) are shown above and below the dashed line, respectively.

hole states obtained in RPA [see Eqs. (43) and (44)] and in ERPA in the lower and upper panels, respectively. The latter is calculated by diagonalizing, at the end of the iterative procedure, the OBDM. All states with $L=0-6$, both in $S=0$ and in $S=1$ spin channels, are used in the calculation of these quantities. However, as mentioned above, RPA breaks down in the $L=3$, $S=1$ channel (as well as in the $L=5$, $S=1$ one), while ERPA solutions are found to be real for all L and S states. We note that the deviations from the HF limit, i.e., $n_h=1$ and $n_p=0$, are greater in ERPA than in RPA. A different result was found in Ref. 32 where, however, several further approximations with respect to the present approach were introduced (see Sec. II). It has to be noticed that the use of quasiboson approximation in the evaluation of RPA matrices is justified only when the HF state does not differ very much from the correlated one. The big deviations found in RPA show that the quasiboson approximation, and thus the standard RPA, is not adequate. As mentioned above, the ERPA occupation numbers deviate from the HF limit more than the RPA ones. However, this is not a difficulty in ERPA since the correlated ground state, rather the HF one, is used as the reference state.

Other useful information about the ground state properties can be obtained by looking at the electron density,

$$\rho(r) = \frac{1}{4\pi}\sum_{\alpha,\beta} \rho(\alpha,\beta)\varphi_{\alpha}(r)\varphi^{*}_{\beta}(r), \tag{47}$$

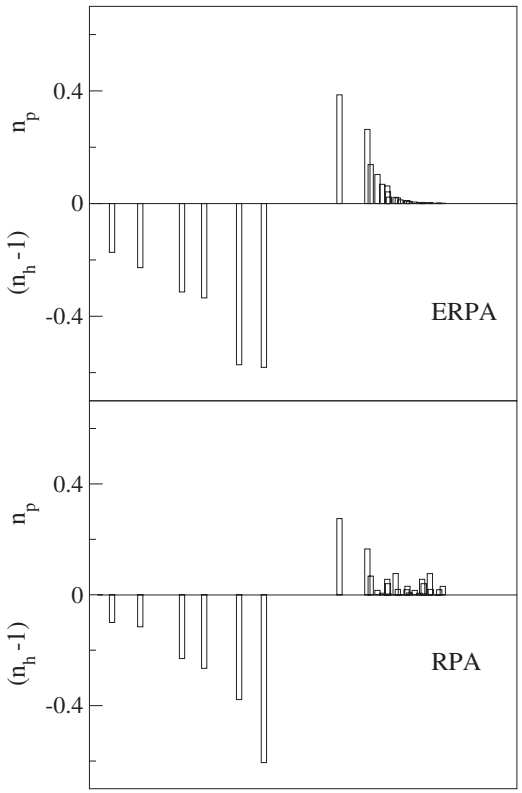

FIG. 5. Occupation numbers n_p for particle states and the opposite of depletion numbers $n_h - 1$ for hole states. ERPA and RPA results are reported in the upper and lower panel, respectively. The ERPA occupation numbers are calculated by diagonalizing, at the end of the iterative procedure, the OBDM, while Eqs. (43) and (44) are used for RPA values.

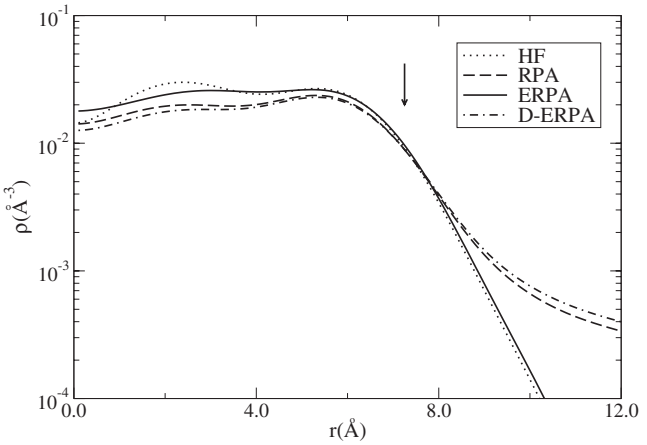

FIG. 6. Electron density ρ for Na_{40} cluster as obtained in HF (dotted line), RPA (dashed line), and ERPA (full line). The D-ERPA result (dotted-dashed line) means the ERPA result when only the diagonal terms of the OBDM are taken. The arrow indicates the radius of the jellium sphere.

where α and β stand for any single HF particle states with wave functions $\varphi_\alpha(r)$ and $\varphi_\beta(r)$ and normalized so that

$$4\pi \int_0^\infty r^2 \rho(r) dr = N_e, \tag{48}$$

where N_e is the number of electrons. In Fig. 6, we show the electron densities calculated in HF (dotted line), RPA (dashed line), and ERPA (full line). Note that in HF, the OBDM is diagonal and one has

$$\rho^{HF}(r) = \frac{1}{4\pi} \sum_h |\varphi_h(r)|^2, \tag{49}$$

where the sum runs only over hole states. Similarly, in RPA, it is still assumed to be diagonal with occupation numbers different from the HF ones [see Eqs. (43) and (44)] and one gets

$$\rho^{RPA}(r) = \frac{1}{4\pi} \sum_\alpha n_\alpha |\varphi_\alpha(r)|^2. \tag{50}$$

We can see that when RPA correlations are included, the electron density in the interior part is smaller than in the HF case while its tail is much longer. On the contrary, the ERPA electron density comes out to be closer to the HF one and, in particular, the tails are almost identical. In Fig. 6, we show also the values (dotted-dashed line, denoted by D-ERPA), which are obtained by taking only the diagonal terms of the OBDM calculated in ERPA. As it is apparent, in this case the electron density gets closer to the RPA one. The HF electron density shows some oscillations in the interior part, which are due to the shell structure and are washed out in the other approaches. However, we underline that HF and ERPA, while having occupation numbers so different from each other, give similar electron densities when the corresponding complete OBDM is used self-consistently.

V. CONCLUSIONS AND OUTLOOK

In conclusion, we have presented an approach (ERPA), going further toward a completely self-consistent RPA. A significant improvement is achieved over the renormalized RPA framework of previous extensions of RPA. In particular, it is less demanding from the point of view of computational resources. In order to test the merits of the new approach, we have applied it to the study of the electronic properties of metal clusters within the jellium approximation. By comparison with the available experimental data, we found that it gives better results than RPA. Sizeable violations of the EWSR are still present in ERPA as in all extensions of RPA proposed until now. As discussed at the end of Sec. III, by enlarging the space of elementary excitations along the lines of Ref. 37 within the present framework, it should be possible to implement a completely self-consistent RPA preserving the EWSR and to overcome the difficulties encountered in Ref. 37. This will be the object of future investigations. As it is clearly pointed out, the applicability of the approach is quite general. Some results shown in the present paper like those on "generalized single particle energies" and on sum rules make us confident that our method will display all its potentialities when applied to the study of atomic nuclei, as we plan to do in the near future.

ACKNOWLEDGMENTS

The authors gratefully acknowledge M. Sambataro and N. Van Giai for helpful discussions. This work makes use of results produced by the PI2S2 Project managed by the Consorzio COMETA, a project co-funded by the Italian Ministry of University and Research (MIUR) within the Piano Operativo Nazionale Ricerca Scientifica, Sviluppo Tecnologico, Alta Formazione (PON 2000–2006). More information is available at http://www.pi2s2.it and http://www.consorzio-cometa.it.

*danilo.gambacurta@ct.infn.it
†francesco.catara@ct.infn.it

[1] D. J. Dean, arXiv:0709-0441v1, Proceedings of the 23rd International Nuclear Physics Conference (INPC 2007), Tokyo, Japan, 2007 (unpublished).
[2] E. Caurier, G. Martinez-Pinedo, F. Nowacki, A. Poves, and A. P. Zuker, Rev. Mod. Phys. **77**, 427 (2005).
[3] P. Navratil, J. P. Vary, and B. R. Barrett, Phys. Rev. C **62**, 054311 (2000).
[4] P. Navratil, V. G. Gueorguiev, J. P. Vary, W. E. Ormand, and A. Nogga, Phys. Rev. Lett. **99**, 042501 (2007).
[5] F. Coester, Nucl. Phys. **7**, 421 (1958); F. Coester and H. Kümmel, *ibid.* **17**, 477 (1960).
[6] H. Kümmel, K. H. Lührmann, and J. G. Zabolitzky, Phys. Rep., Phys. Lett. **36**, 1 (1978).
[7] J. Cížek, J. Chem. Phys. **45**, 4256 (1966).
[8] J. H. Heisenberg and B. Mihaila, Phys. Rev. C **59**, 1440 (1999).
[9] S. C. Pieper and R. B. Wiringa, Annu. Rev. Nucl. Part. Sci. **51**, 53 (2001).
[10] J. Carlson, Phys. Rev. C **36**, 2026 (1987).
[11] B. S. Pudliner, V. R. Pandharipande, J. Carlson, S. C. Pieper, and R. B. Wiringa, Phys. Rev. C **56**, 1720 (1997).
[12] T. Otsuka, T. Mizusaki, and M. Honma, J. Phys. G **25**, 699 (1999).
[13] D. Vautherin and D. M. Brink, Phys. Rev. C **5**, 626 (1972).
[14] D. J. Rowe, *Nuclear Collective Motion* (Methuen, London, 1970).
[15] P. Ring and P. Schuck, *The Nuclear Many-Body Problem* (Springer-Verlag, Berlin, 1980).
[16] M. Grasso, F. Catara, and M. Sambataro, Phys. Rev. C **66**, 064303 (2002).
[17] D. Beaumel and Ph. Chomaz, Ann. Phys. (N.Y.) **213**, 405 (1992).
[18] M. Sambataro and F. Catara, Phys. Rev. C **51**, 3066 (1995).
[19] M. Sambataro and J. Suhonen, Phys. Rev. C **56**, 782 (1997).
[20] F. Catara, Ph. Chomaz, and N. Van Giai, Phys. Lett. B **233**, 6 (1989).
[21] E. G. Lanza, M. V. Andres, F. Catara, Ph. Chomaz, and C. Volpe, Nucl. Phys. A **613**, 445 (1997).
[22] C. Volpe, Ph. Chomaz, M. V. Andres, F. Catara, and E. G. Lanza, Nucl. Phys. A **647**, 246 (1999).
[23] D. Gambacurta, M. Sambataro, and F. Catara, Phys. Rev. C **73**, 014310 (2006).
[24] M. Sambataro and N. Dinh Dang, Phys. Rev. C **59**, 1422 (1999).
[25] D. Gambacurta, M. Grasso, F. Catara, and M. Sambataro, Phys. Rev. C **73**, 024319 (2006).
[26] J. Dukelsky and P. Schuck, Nucl. Phys. A **512**, 466 (1990).
[27] D. Janssen and P. Schuck, Z. Phys. A: Hadrons Nucl. **339**, 43 (1991).
[28] A. Klein, N. R. Walet, and G. Do Dang, Nucl. Phys. A **535**, 1 (1991).
[29] D. Karadjov, V. V. Voronov, and F. Catara, Phys. Lett. B **306**, 197 (1993).
[30] F. Catara, N. Dinh Dang, and M. Sambataro, Nucl. Phys. A **579**, 1 (1994).
[31] J. Dukelsky and P. Schuck, Phys. Lett. B **387**, 233 (1996).
[32] F. Catara, G. Piccitto, M. Sambataro, and N. Van Giai, Phys. Rev. B **54**, 17536 (1996).
[33] F. Catara, M. Grasso, G. Piccitto, and M. Sambataro, Phys. Rev. B **58**, 16070 (1998).
[34] A. A. Raduta, C. M. Raduta, A. Faessler, and W. A. Kaminski, Nucl. Phys. A **634**, 497 (1998).
[35] F. Krmpotić, E. J. V. de Passos, D. S. Delion, J. Dukelsky, and P. Schuck, Nucl. Phys. A **637**, 295 (1998).
[36] F. Šimkovic, A. A. Raduta, M. Veselsky, and A. Faessler, Phys. Rev. C **61**, 044319 (2000).
[37] M. Grasso and F. Catara, Phys. Rev. C **63**, 014317 (2000).
[38] W. Ekardt, Phys. Rev. B **31**, 6360 (1985); W. Ekardt, *ibid.* **32**, 1961 (1985).
[39] M. Brack, Rev. Mod. Phys. **65**, 677 (1993).
[40] C. Guet and W. R. Johnson, Phys. Rev. B **45**, 11283 (1992).
[41] J. Toivanen and J. Suhonen, Phys. Rev. Lett. **75**, 410 (1995).
[42] V. Rodin and A. Faessler, Phys. Rev. C **66**, 051303(R) (2002).
[43] D. J. Rowe, Phys. Rev. **175**, 1283 (1968).
[44] D. J. Thouless, Nucl. Phys. **21**, 225 (1960).
[45] W. A. Heer, Rev. Mod. Phys. **65**, 611 (1993).
[46] J. Borggreen, P. Chowdhury, N. Kebaïli, L. Lundsberg-Nielsen, K. Lützenkirchen, M. B. Nielsen, J. Pedersen, and H. D. Rasmussen, Phys. Rev. B **48**, 17507 (1993).
[47] H. Lenske and J. Wambach, Phys. Lett. B **249**, 377 (1990).
[48] W. D. Knight, K. Clemenger, W. A. de Heer, and W. A. Saunders, Phys. Rev. B **31**, 2539 (1985).
[49] M. Madjet, C. Guet, and W. R. Johnson, Phys. Rev. A **51**, 1327 (1995).
[50] F. Alasia, Ll. Serra, R. A. Broglia, N. Van Giai, E. Lipparini, and H. E. Roman, Phys. Rev. B **52**, 8488 (1995).